VĚDECKÉ SPISY VYSOKÉHO UČENÍ TECHNICKÉHO V BRNĚ

Edice PhD Thesis, sv. 338

ISSN 1213-4198

Ing. Karel Čermák

Optimization of Optoelectronic Velocity Measuring Devices Based on Spatial Filtering Method

BRNO UNIVERSITY OF TECHNOLOGY

Faculty of Electrical Engineering and Communication

Institute of Radio Electronics

Ing. Karel Čermák

OPTIMIZATION OF OPTOELECTRONIC VELOCITY MEASURING DEVICES BASED ON SPATIAL FILTERING METHOD

OPTIMALIZACE OPTOELEKTRONICKÝCH MĚŘIČŮ RYCHLOSTI ZALOŽENÝCH NA METODĚ PROSTOROVÉ FILTRACE

SHORT VERSION OF PH.D. THESIS

Study field: Electronics and Communications

Supervisors: Ing. Aleš PROKEŠ, Ph.D.
Prof. Dr. Friedemann MOHR (UAS Pforzheim)

Opponents: Prof. Ing. Čestmír Vlček, CSc.
Doc. Ing. Karel Novotný, CSc.

Presentation date: September 16, 2005

KEYWORDS

Transversal velocity measurement, Spatial Filtering Method (SFM), SFM based velocity measurement, surface structure analysis, spatial filter adaptation on the surface properties, dual differential spatial filter, optimization of SFM based devices, spatial filter realized on CCD or CMOS chip, correlation method, speckle method, laser Doppler method.

KLÍČOVÁ SLOVA

Transverzální měření rychlosti, metoda prostorové filtrace (SFM), měření rychlosti založené na metodě prostorové filtrace, analýza povrchové struktury, přizpůsobení prostorového filtru vlastnostem měřeného povrchu, dvojitý diferenciální prostorový filtr, optimalizace zařízení založených na SFM, realizace prostorového filtru na čipu CCD nebo CMOS, korelační metoda, metoda využívající „zrnitosti“ laserové záření, laserová Dopplerovská metoda.

The thesis is available at the Science department of Dean's office FECT BUT in Brno, Údolní 53, Brno, 602 00

ISBN 80-214-3031-1
ISSN 1213-4198

CONTENTS

1 INTRODUCTION

1.1 PROBLEM FORMULATION

Optical velocity measuring devices might be divided into two groups according to the relative angle between the observation direction and the movement direction of the object:

- devices for longitudinal velocity measurement (Fig. 1.1a),
- devices for transversal velocity measurement (Fig. 1.1b).

In the following figure, point P designates the velocity-measuring device and point O represents the object position.

Fig. 1.1. (a) Measurement setup for longitudinal velocity measurement. (b) Measurement setup for transversal velocity measurement.

The best-known *longitudinal* measurement concepts are based on one of the following methods [16]:

- triangulation method,
- laser radar employing pulse and modulation-phase method,
- interferometric method [45].

A specific implementation of the latter, the so-called laser vibrometer, is optimized for measuring vibrations from non-cooperating (i.e., non-reflecting) surfaces and has come to a high perfection in the last years [46].

Devices for *transversal* measurement can be attributed to either of the following methods:

- correlation method [42], [26],
- speckle method [23],
- laser Doppler method [53], [50]
- **Spatial Filtering Method (SFM)** [3], [22].

In the next section the principle of laser Doppler method and spatial filtering method (SFM) will be described.

1.2 LASER DOPPLER VELOCITY METER (LDV)

The first device based on the principle of Laser Doppler Anemometry (LDA) was constructed in 1964. Initially, the concept was used for gas or particle flow measurement. Later, the method was enhanced to enable measurement of the surface velocity of solid objects. Commercial companies designate their surface velocity meters - Laser Doppler Velocimeters (LDV). This kind of instrument generates an interference figure (serving the role of a spatial filter) on the object surface by making two laser beams intersect under a very small angle.

The level of the light intensity scattered by the surface is given by the correlation of the spatial filter and the surface spatial frequency characteristics. The fringe spacing g_x is given by [50]

$$g_x = \frac{\lambda}{2\sin\varphi}, \tag{1.1}$$

where λ is the wavelength of the laser and φ is the half-angle between the two crossing laser beams. For better understanding of the method let us consider the moving surface as being completely dark and absorbing except for a single bright dot. While this dot is moving through the observation field, its varying illumination produces alternating bright and dark flashes occurring with a velocity-dependent frequency f_D.

The dependency of f_D on the velocity v_o is described by the Doppler formula

$$f_D = \frac{v_o}{g_x}. \tag{1.2}$$

1.3 SPATIAL FILTERING METHOD (SFM)

1.3.1 The basic concept

The use of spatial filters for measuring the velocity of moving objects was first mentioned about 70 years ago [28]. This method utilizes the intensity modulation caused by observing a spatial filter, behind which a bright object is moving laterally to the filter lines. The simplest spatial filter can be formed by a row of slots as shown in Fig. 1.2a. In this arrangement the moving object consists of single strip moving from left to right and, thus, alternately shading the transmitting openings in the mask.

The faster the strip moves in the sensing plane, the faster gets the blinking frequency of the signal passing through the grating and vice versa. In other words, the maximum of the power spectrum, which is received by the photo detector, is settled at the frequency f_o when the velocity of the moving object is v_o. The frequency f_o, obtained from the photo-detector can be computed as

$$f_o = \frac{v_o M}{g_x}, \tag{1.3}$$

where g_x is the grid constant the spatial filter. The M is a magnification factor of the optical system, if any.

The signal occurring at the output of the photo-diode is shown in Fig. 1.2b. The upper dashed line denotes the light intensity s_{1max} (t) detected without the spatial filter. After placing the spatial filter between the light source and the photo-detector the intensity drops to half of its previous value. Moving the opaque strip along the x-axis with a constant velocity v_o leads finally to a periodic shading of the mask thus leading to the saw-tooth-shaped intensity modulation depicted (full line).

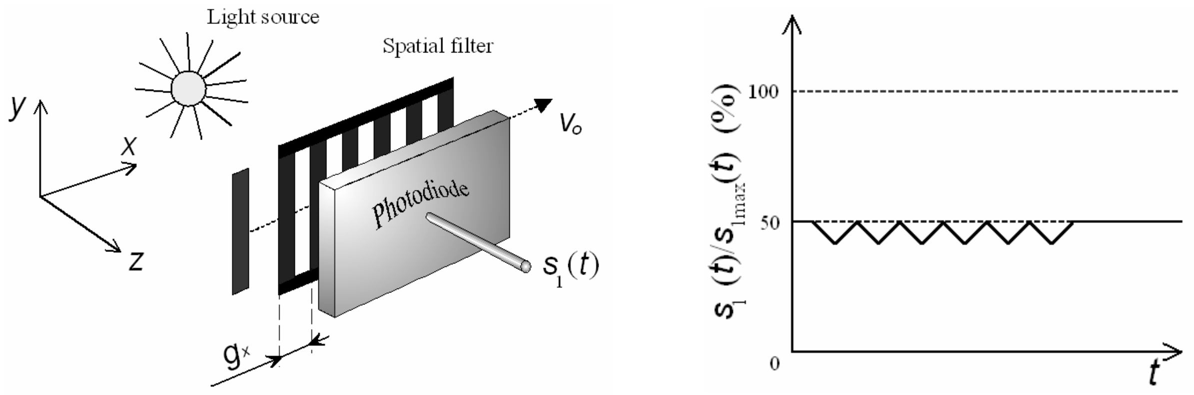

(a) (b)

Fig. 1.2. (a) Principle of spatial filtering method. (b) Normalized signal at the output of the photo-detector.

1.3.2 Spatial filtering using CCD detectors

CCD line detectors are composed of closely adjacent individual photo-detectors and thus, are very similar to the arrangements discussed so far. It is not astonishing that soon after the advent of CCD chips the idea of using these not only as a photo detector but also as a spatial filter appeared. Astech was one manufacturer that became known for developing measuring devices exploiting the potential of CCD chips. With these, the differential DC free signal is produced in a manner shown in Fig. 1.3.

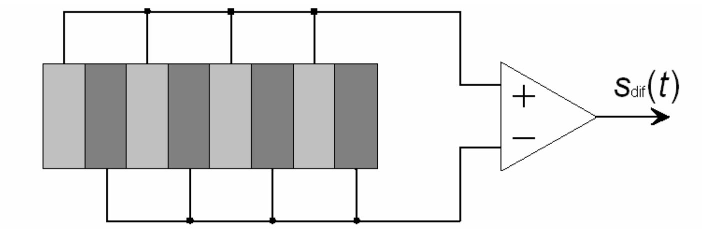

Fig. 1.3. Reading the differential signal from CCD chip.

1.4 RÉSUMÉ

The transversal methods for velocity measurement can be divided into those using monochromatic coherent light source (laser) and those using a wide band incoherent source of light (white light). Both the Laser Doppler Velocimeter (LDV, which uses laser light) and the method that we call Spatial Filter Method (SFM, which uses incoherent light) are based upon utilization of the spatial filter as the fundamental measurement concept. They differ only in the way how and at which place of the measuring system the superposition of the spatial filter and the surface structure is performed: With the LDV this is in the illumination area, directly on the moving surface while with the SFM method it is in the image area close to the detectors. The information about the velocity of the moving surface is given by formula (1.3).

1.5 AIMS OF THE DISSERTATION

Several realisation schemes of the spatial filters are known. Among these are: differential prisms spatial filters, fiber based differential spatial filters, LCD spatial filters or spatial filters created directly by the periodic structure of CCD or CMOS chips.

Another implementation is the laser Doppler concept where the required periodic reference structure is implemented in the illuminating part of the system.

All approaches were conceived to achieve low-cost yet still accurate devices capable of measuring velocities from millimetres up to hundreds of meters per second. However, all known implementations have the common property to use a fixed reference filter while the spatial spectrum characteristics of the surface can vary over a broad range due to e.g. roughness, colour, scattering efficiency etc. which are characteristic for every surface.

Goals of the research: Therefore, if the SFM based velocity meter is to be really universal, it should be designed for adaptability on the measured surface. The aim of the research is to determine which surface characteristics require matching, and how this matching can be realized by spatial filter and detector circuitry.

Prospective advantages:

- setting the optimization criteria for the spatial filter,
- enabling velocity measurement also with periodic structures (which so far constitutes a problem),
- decreasing the measurement uncertainty.

2 ADAPTIVE SPATIAL FILTER PROPOSAL

2.1 MATHEMATICAL DESCRIPTION OF THE SIGNAL GENERATION PROCESS

2.1.1 Signal generation process using single spatial filter

With the spatial filtering based method (SFM), the target surface is projected on the reference filter, and the intensity transmitted is detected by a photo-detector. The reference filter normally is a "two-in-one" arrangement providing two output signals in counter-phase cf. Fig. 1.3. Subtraction of both yields a bias-free output signal $s_{dif}(t)$ suitable for further processing. Mathematically, the signal in *one* channel is, for a stationary object, described as [43]

$$s = K\int_{-\infty}^{+\infty}\int_{-\infty}^{+\infty} i(x,y)\,h(x,y)\,dx\,dy \tag{2.1}$$

with K denoting the sensitivity of the photo-detector, $i(x,y)$ the light intensity distribution of the surface and $h(x,y)$ the light transmittance distribution of the spatial filter. The output s of the photo-detector is described as the integral of the light intensity i of the surface passing through the spatial filter. Assuming uniformly moving surface in x-axis with velocity v_o we get

$$s(t) = K\int_{0}^{L_y}\int_{0}^{L_x} i(x - v_o t, y)\,h(x,y)\,dx dy\,, \tag{2.2}$$

where L_x and L_y is the length and width of the spatial filter, respectively. Taking into consideration only the distribution in x-axis (a one-dimensional approach with y being a constant), one obtains

$$s(t) = K\int_{0}^{L_x} i(x - v_o t)\,h(x)\,dx\,. \tag{2.3}$$

The frequency spectrum of the signal received at the photo-detector is then given by the convolution theorem of Fourier transformation [29]

$$S(f) = \left(-\frac{1}{v_o}\right) I\left(-\frac{f}{v_o}\right) H\left(\frac{f}{v_o}\right), \tag{2.4}$$

where

$$I\left(\frac{f}{v_o}\right) = \int_{0}^{L_x} i(x)\, e^{\left(j2\pi\frac{f}{v_o}x\right)} dx \tag{2.5}$$

and

$$H\left(\frac{f}{\mathrm{v}_o}\right)=\int_0^{L_x} h(x)e^{\left(j2\pi\frac{f}{\mathrm{v}_o}x\right)}dx \quad (2.6)$$

are the spatial frequency spectra of the surface texture and the grating, respectively. Here is the spatial frequency f_s (m^{-1}) is expressed as a number of periods per unit length and can be computed as

$$f_s=\frac{f}{\mathrm{v}_o}. \quad (2.7)$$

2.1.2 Signal generation process using differential spatial filter “two-in- one”

The signal at the photo-detector output $s_1(t)$ of the first half of the differential spatial filter “two-in-one” cf. Fig. 1.3 can be described as

$$s_1(t)=K\int_0^{L_x} i(x-v_o t)h_1(x)dx, \quad (2.8)$$

where h_1 denotes the light transmittance distribution of the first spatial filter. Correspondingly, the signal at the photo-detector output $s_2(t)$ of the second half of the differential spatial filter “two-in-one” reads

$$s_2(t)=K\int_0^{L_x} i(x-v_o t)h_2(x)dx, \quad (2.9)$$

where h_2 is light transmittance distribution of the second spatial filter. The signal $s_{\text{dif}}(t)$, which is obtained after subtracting the signals $s_1(t)$ and $s_2(t)$ is

$$s_{\text{dif}}(t)=s_1(t)-s_2(t). \quad (2.10)$$

2.2 SPATIAL FILTER PROPERTIES

In this section, the spatial filter properties are described. There are several potential realizations, which have already been discussed in section 1.3. From these, we take as a basis for our discussions to come the spatial filter realization on the CCD chip. We denote the number of periods N, the period length g_x and the spatial filter width L_y, cf. Fig. 2.1.

For constant g_x, the ideal rectangular spatial filter can be described as

$$h_1(x)=L_y\sum_{n=0}^{N-1}u(x-ng_x), \quad (2.11)$$

where

$$u(x) = \sigma(x) - \sigma\left(x - \frac{g_x}{2}\right) \tag{2.12}$$

and $\sigma(x)$ denotes the Heaviside function, i.e. $\sigma(x) = \begin{cases} 0 & x < 0 \\ 1 & x \geq 0 \end{cases}$.

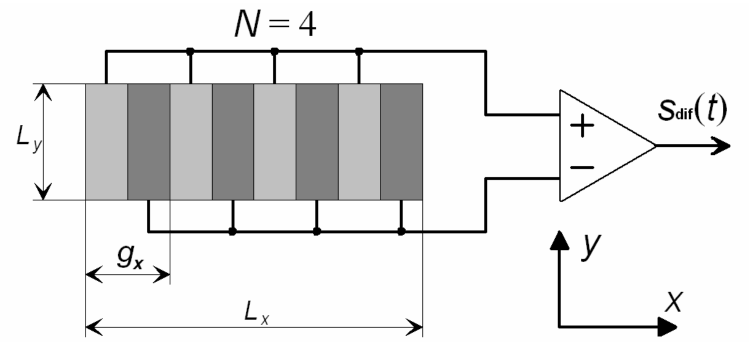

Fig. 2.1. The differential spatial filter realization using a CCD chip.

The second one is in counter-phase

$$h_2(x) = L_y \sum_{n=0}^{N-1} u\left[x - \left(n + \frac{1}{2}\right) g_x\right]. \tag{2.13}$$

However, in order to simplify the analysis for the moment, we approximate both characteristics with pure harmonic functions. Then, we get for h_1 and h_2, respectively,

$$h_1(x) = \frac{1}{2} w_x L_y \left[1 + \sin\left(\frac{2\pi}{g_x} x\right)\right] \tag{2.14}$$

and

$$h_2(x) = \frac{1}{2} w_x L_y \left[1 + \sin\left[\left(\frac{2\pi}{g_x} + \pi\right) x\right]\right], \tag{2.15}$$

where $w_x(x)$ denotes the rectangular windowing function of length L_x,

$$w_x(x) = \begin{cases} 1 & 0 \leq x \leq L_x \\ 0 & \text{else} \end{cases}. \tag{2.16}$$

Even though our restriction to simple harmonic functions is for simplification only, it should be mentioned that real systems are described by transmission functions with rounded edges, i.e., their mathematical description lies somewhere between harmonic and rectangular [51].

The relation between the generated main lobe maximum frequency f_o and the velocity v_o is described by (1.3). According to (1.3) f_o depends on the optical magnification factor M and on the spatial filter period length g_x. This formula provides exact results for an infinite number of spatial filter periods, $N \rightarrow \infty$. In this case the position of the main lobe spatial frequency maximum f_M can be computed as

$$f_M = \frac{1}{g_x}. \qquad (2.17)$$

For a real case the number of periods is finite. This limitation leads to the frequency shift of the main lobe maximum f_M. However, it can be calculated exactly for every number of spatial filter periods and for a given shape of the spatial filter. Further, the exact relation between the number of spatial filter period N and the relative bandwidth B_M of the main lobe was computed and can be described as

$$\frac{B_M}{f_M} = \frac{2}{N}, \quad \text{for } N > 1. \qquad (2.18)$$

2.3 SURFACE AND ITS ANALYSIS AND DESCRIPTION

The investigated surfaces have the following properties: with increasing width of the integrated surface increases the intensity of the amplitude spectrum, while the growth rate varies between linear and square root. The increase can be approximated with square root function the better, the more stochastic the surface is. The spectral pattern caused by a periodic character of the structure can considerably impair the measurement or even make it virtually impossible. It follows that some intelligent suppression of the harmonic structure is required.

The simulations shows also that the $f_{S\text{-}3dB}$ frequency for all the investigated surfaces can be found in the range of $f_{S\text{-}3dB} = 0.8 \div 1.1$ mm $^{-1}$. From this point on the intensity decreases with about -20dB/dec. Amplitude spectra of analysed surfaces can also be approximated with exponential function. This corresponds with the in [38] presented results.

2.4 CRITERIA FOR PERIODIC STRUCTURE SUPPRESSION

All real structures can be considered as quasi-stochastic or quasi-periodic structures, while strongly periodic structure can leads to causing a permanent measurement error. In this chapter the optimization criteria for the differential spatial filter adaptation on the periodic surface structure are described, while the spatial filter approximated with rectangular function is considered cf. (2.11) and (2.13). The proposed results can be used for the optimal spatial filter setting if strongly periodic structures occur. The idea of elimination of the real surface harmonic components is based on the following formula

$$f_{SF0} = \frac{m \cdot f_M}{N}, \; m = 0,1,2,3...; \; m \neq N, 3N, 6N, 9N, ..., \tag{2.19}$$

where f_{SF0} is that spatial frequency, where the differential spatial filter transfer function approaches zero. N is the number of spatial filter periods and f_M is the spatial frequency of the main lobe maximum cf. (2.17).

If we want to eliminate a periodic structure on the surface at the spatial frequency f_s, the following condition must be satisfied

$$f_s = f_{SF0}. \tag{2.20}$$

This can also be formulated in the spatial domain for the whole length L_x of the spatial filter

$$L_x = m \cdot \frac{1}{f_{sx}} = m \cdot l_x, \; m = 1,2,3.... \tag{2.21}$$

Another way of eliminating periodic structure is to optimize the width of the spatial filter L_y (see Fig. 2.1) on the periodic structure of the material. This is described by the following formula

$$L_y = m \cdot \frac{1}{f_{sy}} = m \cdot l_y, \; m = 1,2,3..., \tag{2.22}$$

where f_{sy} designates the spatial frequency to be suppressed and l_y the length of the surface period in y-axis direction. This formula is based on the fact that the spatial filter integrates the surface intensity in the y-axis as well.

How successful the periodic structure suppression process will be depends on the mark to space ratio (MSR) of the frequency f_{sy}. Mark to space ratio can be computed as

$$MSR = \frac{o_M}{l_y} = \frac{l_y - o_S}{l_y}, \tag{2.23}$$

where the o_M is the length of the mark and o_s is the length of the space.

Now, the case of chequered material structure is considered. That kind of structure can be found in most textile materials. These periodic structures have the same frequency (period) in vertical and horizontal direction and 180° columns phase shift. The task is to eliminate the periodic structure. The maximal suppression of the periodic structure will fully succeed only if the columns phase shift is 180° and only for symmetrical structures. With non-symmetrical structures the grade of suppression depends on non-symmetric factor. The higher is the non-symmetry the lower the suppression of the periodic structure.

The suppression of periodic structure in the x-axis (horizontally) is based on (2.21). As one can easily imagine the suppression will have 100% efficiency only for periodic structures with line-like frequency spectrum.

2.5 IMPROVING THE SPATIAL FILTERING METHOD

2.5.1 Dual differential spatial filter

The block diagram of dual differential spatial filter (DDSF) is shown in Fig. 2.2. The DDSF is composed of two differential spatial filters ("two-in-one") and could be realised e.g. on the CCD or CMOS camera chip. The idea of DDSF is based on multiple autocorrelation between two differential spatial filters. In order to explain the principle of the DDSF, let us simplify the real scheme shown in Fig. 2.2 down to the situation shown in Fig. 2.3. In this picture each differential spatial filter is replaced with one point. The point "a" represents the upper differential spatial filter producing the signal $s_{\mathrm{dif1}}(t)$ and the point "b" substitutes the lower differential spatial filter producing the signal $s_{\mathrm{dif2}}(t)$. These two signals are subtracted. On the output of the differential amplifier the dual differential spatial filtration product $s_{\mathrm{ddif}}(t)$ can be measured.

These two differential spatial filters and moving surface in x-axis direction are considered now. The relation between them can be described as

$$\begin{aligned} r_{\mathrm{a-b}}(\Delta x) &= \int_{-\infty}^{\infty} [i_{\mathrm{a}}(x) - i_{\mathrm{b}}(x)][i_{\mathrm{a}}(x+\Delta x) - i_{\mathrm{b}}(x+\Delta x)]dx \\ &= \int_{-\infty}^{\infty} i_{\mathrm{a}}(x)i_{\mathrm{a}}(x+\Delta x) - i_{\mathrm{b}}(x)i_{\mathrm{a}}(x+\Delta x) - i_{\mathrm{a}}(x)i_{\mathrm{b}}(x+\Delta x) + i_{\mathrm{b}}(x)i_{\mathrm{b}}(x+\Delta x)dx \\ &= r_{\mathrm{aa}}(\Delta x) + r_{\mathrm{bb}}(\Delta x) - r_{\mathrm{ab}}(\Delta x) - r_{\mathrm{ba}}(\Delta x). \end{aligned} \tag{2.24}$$

The formula (2.24) consists of four terms. All the expressions i.e. $r_{\mathrm{aa}}(\Delta x)$, $r_{\mathrm{bb}}(\Delta x)$, $r_{\mathrm{ab}}(\Delta x)$ and $r_{\mathrm{ba}}(\Delta x)$ depend on the autocorrelation level of the surface. For the surface with white noise character all terms equal zero. On the other hand, if the surface includes at least small autocorrelation and that is the case with most of the real surface structures, then all the expressions become non-zero. For the correct function of the dual differential filter the expressions $r_{\mathrm{ab}}(\Delta x)$ and $r_{\mathrm{ba}}(\Delta x)$ are important. These expressions are subtracted of the main expressions $r_{\mathrm{aa}}(\Delta x)$ and $r_{\mathrm{bb}}(\Delta x)$. They will cause the periodic-like structure attenuation.

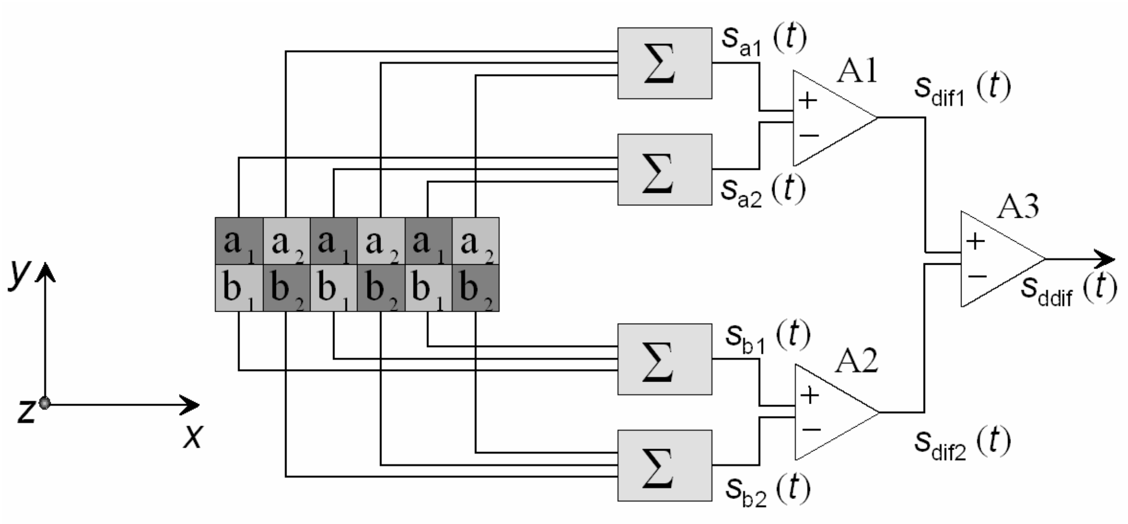

Fig. 2.2. Dual differential spatial filter.

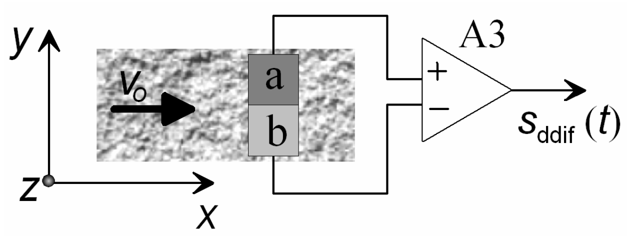

Fig. 2.3. Dual differential spatial filter – the solution for the advanced periodic structure suppression.

Computing subtractions, one obtains two differential filtering products. These products are denoted as s_{1dif} and s_{2dif}

$$s_{1\mathrm{dif}} = s_{\mathrm{a}1}(t) - s_{\mathrm{a}2}(t) \tag{2.25}$$

and

$$s_{2\mathrm{dif}} = s_{\mathrm{b}1}(t) - s_{\mathrm{b}2}(t). \tag{2.26}$$

The dual differential filtration product s_{ddif} is then obtained as

$$s_{\mathrm{ddif}} = s_{\mathrm{dif1}}(t) - s_{\mathrm{dif2}}(t). \tag{2.27}$$

2.5.2 Dual differential spatial filter – setting the optimal width L_y

Stochastic surface

In this section the optimal spatial filter width setting is discussed. For our further discussion the spatial filter realized on CCD matrix is considered.

Firstly, the surface is considered to be ideally stochastic white noise. The mean value μ of the white noise summation process for certain width L_y of the spatial filter can be described as

$$\mu(L_y) = \mu(1)L_y, \tag{2.28}$$

where $\mu(1)$ is the mean value of the stochastic process for L_y = 1. The standard deviation then

$$\sigma(L_y) = \sigma(1)\sqrt{L_y}, \tag{2.29}$$

where $\sigma(1)$ is the standard deviation of the stochastic process for $L_y = 1$.

The contrast can be computed as the ratio between standard deviation and mean

$$k(L_y) = \frac{\sigma(1)}{\mu(1) \cdot \sqrt{L_y}}. \tag{2.30}$$

The width of the spatial filter can be computed as

$$L_y = M \cdot p_y, \tag{2.31}$$

where p_y is the real width of one single pixel and M is a positive integer number - the number of pixels. According to formula (2.30) thin spatial filter should be preferred.

Quasi-stochastic and quasi-periodic surface structures

In this group almost all real surfaces can be included. As described above, the dual differential filter improves the filtration product the better the wider the surface auto-correlation function. However, for further investigation only the frequency components for $f_s \neq 0$ are interesting. Therefore, the DC (mean) can be removed - the auto covariance function was computed. It was determined, that the steepness of the auto-covariance function decreases with increasing roughness of the material. According to (2.24) the suppressing factor of the dual differential filter depends on the correlation between the surfaces scanned by each differential spatial filter. Therefore, the suppression of the un-required periodic character will be the better the wider the auto-covariance function.

Second important factor for the suppression level of the un-required periodic structures is the width of the spatial filter L_y. According to (2.38) the L_y should be chosen as thin as possible in order to gain the signal contrast. However, the simulations show, that for real surfaces by shrinking the L_y to about $L_y = 0.1 \div 0.3$mm, the curves become flat top. That means that the contrast remains nearly the same with further L_y shrinking.

One can conclude that with almost all real surfaces the width of the spatial filter L_y should be chosen as thin as possible. The exception might be chequered surface structures with 180° columns phase shift. The main limitation factor is the sensitivity of the photodiode, CCD or CMOS sensor. The application of the dual differential filter will be the more profitable the higher the auto-covariance of the surface.

3 PRACTICAL TESTS AND MEASUREMENTS

In order to verify the theoretical computations and simulations, the practical experiments on commercial and self-constructed device were carried out. The self-constructed SFM device was based on a high speed CCD camera.

The measurement with the commercial device confirmed the predicted problems, which can occur during the measurement with typical non-adaptive device based on spatial filtering method. The experiments have confirmed the main lobe maximum frequency shift due to different surface structures of measured materials. This shift was mainly caused by surfaces exponential-like decrease of the amplitude spectrum.

Then in this thesis proposed dual differential spatial filter was realized on above mentioned measurement setup based on a high speed CCD camera. The block diagram of the measurement setup is shown in Fig. 3.1.

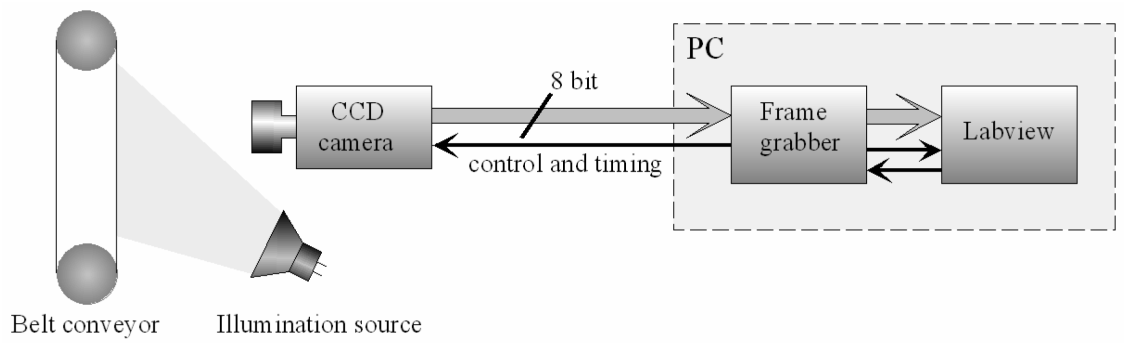

Fig. 3.1. Measurement setup with high speed CCD camera.

In Fig. 3.2, as an example, the comparison of the simulated and measured results for chequered surface is shown. In Fig. 3.2a the surface used as an input for the simulation is depicted. Fig. 3.2b shows a snapshot of the measured surface taken by the high speed CCD camera. If one compares the simulation (cf. Fig. 3.2c) and measurement results (cf. Fig. 3.2d), it is obvious, that the filtration product of the optimally adapted DDSF provides in both cases correct maximum and suppresses the undesirable periodic surface structure distinctly. In Fig. 3.2c the averaged spectra obtained by multiplication of the surface structure and the spatial filter are depicted. The spectra shown in Fig. 3.2d were computed from data collected by the high speed CCD camera. The mean velocity of the measured surface was $v_b = 169.20$ mm/s, which corresponds to the mean main lobe frequency maximum $f_o = 252$ Hz, cf. (1.3).

The measurement confirmed the simulations carried out in chapter two. The dual differential filter suppresses the side lobes and the periodic structure the better, the thinner the spatial filter width and the wider the auto-covariance function of the measured material.

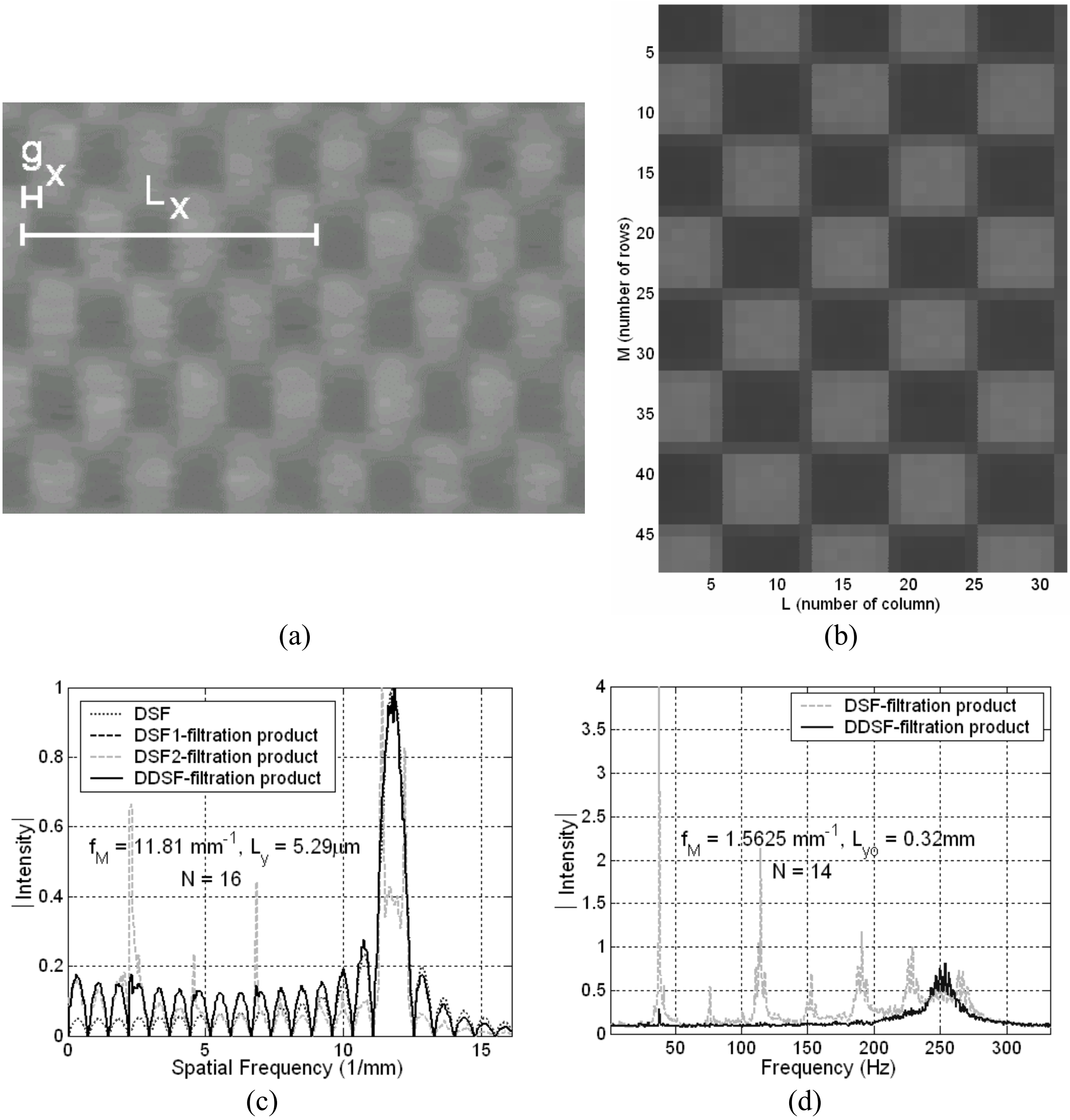

Fig. 3.2. (a) The surface used for the simulation, (b) the simulation results. (c) The by high-speed CCD camera measured surface, (d) the measurement results.

4 CONCLUSION

The aim of the dissertation thesis was to improve the understanding of velocity measurement devices based on the spatial filtering method, especially under the viewpoint of recent developments in electronic technology such as CCD and CMOS. One problem that became obvious from our investigations was that by measuring periodic-like surface structures a permanent measurement error can occur. Another problem is the insufficient suppression of the side lobes especially in the region of lower spatial frequencies [15].

Our investigations started with an algebraic description of the signal generation process. The mathematics derived is based upon the mutual interaction of two factors: the characteristics of the spatial filter and the properties of the measured surface cf. formula (2.1). In the simplest case, the output frequency representing the desired measurand is generated by the imaging of the moving surface under investigation onto a reference mask (serving as the spatial filter) and by observing the transmitted intensity through a photo-detector.

Therefore, an analysis and description of the spatial filter properties was done first. Computer simulations confirmed the assumptions made, and also extended results were presented in [33]. It was also confirmed that the number of the spatial filter periods has to be chosen as high as possible. Then, in a frequency-domain oriented view, the bandwidth and also the shift of the maximum of the main lobe is minimised, which makes the measurement more accurate. The main lobe maximum shift can be considered a systematic error and is not critical. It can be calculated exactly for every number of spatial filter periods and for a given shape of the spatial filter.

In a second step, a detailed analysis of the surface characteristics of selected materials was made in order to classify and describe the surface properties. This step of our investigations was intended to provide information for determining the requirements for an optimum match between the spatial filter characteristics – which can be tuned artificially - and the characteristics of the surface – which in most cases is given and cannot be influenced by the user. It turned out that with the chosen set of measured and analyzed surface structures, the spatial spectrum decreases with increasing frequency. The roll-off is such that the spectrum can be well approximated with an exponential function. One astonishing result was that the cut-off frequency lies in the region of $f_{S\text{-}3dB} = 0.8 \div 1.1\ \mathrm{mm}^{-1}$ for all investigated quasi-stochastic materials.

Based on the investigations described above as steps one and two, the optimisation criteria for the suppression of undesired artefacts from periodic surface structures were derived.

First, the undesirable periodic structure can be eliminated to a certain degree by optimizing the spatial filter properties in x-axis direction, cf. formula (2.19). The minimum-transmission spatial filter frequencies should be tuned so as to coincide with the periodic structure maxima. Hereby the disturbing maxima, which are located outside the main lobe, can be suppressed. We should also make sure, according to (2.21) that the whole number of periods of the periodic structure fit into the length of the spatial filter L_x. The suppression becomes optimal only for a periodic structure with unity mark-space ratio ($MSR = 1$).

Influences of the width of the mask (y-axis) have also been considered. It was shown that an optimum periodic-structure-suppression of the spatial filter in y-axis is possible only for chequered structures.

There is also another point of view for choosing the optimal spatial filter width L_y - the signal contrast. According to (2.30) the L_y should be, for white noise-like surface structure, chosen as thin as possible in order to gain the signal contrast. For investigated real surface structures the contrast increases with the decreasing width of the integrated surface as well, however, by shrinking the L_y to about $L_y = 0.1 \div 0.3$mm, the curves become flat top. That means that the contrast remains nearly the same by further shrinking of L_y. The flat top is the wider the wider the auto-covariance function of the surface.

A more sophisticated way of suppressing side lobes and periodic structures uses the proposed dual differential spatial filter (DDSF). This filter is based on a multiple auto-correlation principle. The maximum efficiency of the dual differential spatial filter can be obtained for minimum width L_y of both differential spatial filters. For structured field photo-detectors spatial filter the width of one pixel is suggested.

Combining the dual differential spatial filter with the optimization criteria, a suppression of non-required side lobes and periodic structures can be achieved at almost all real surfaces. Following this concept, a very accurate device for velocity measurement can be constructed. Such a device is able to measure virtually any surface with the highest possible accuracy, the only exception being that of glossy materials.

The presented results are confirmed by theoretical simulations and practical experiments. Practical experiments were based on an analyzed commercial device and also on a self-constructed measurement setup using a high speed CCD camera.

The measurement accuracy of non-contact velocity measuring devices based on spatial filtering method is ever increasing. Three concepts of spatial filtering compete nowadays. The LDV method, the off-chip SFM and the on-chip SFM:

The off-chip method offers measurement of very high velocities. This is due to the use of very fast single-area photodiodes combined with a suitable mask. However, with this concept, the adaptation to the surface is naturally limited.

The on-chip method, which exploits the periodic structure of a CCD (or similar) device, offers the potential of an adaptation to the surface, but the maximum velocity is limited by the maximum frame rate of the CCD or CMOS chip. Constructing the device using CCD or CMOS chip for measuring at very high velocities is still too expensive. The possible solution of how to get all advantages of the off-chip and the on-chip realization is to use a field diodes array with proper circuitry according to Fig. 2.2 instead of CCD or CMOS chip. This could be an inspiration for further research in this interesting field.

REFERENCES

[1] ACHWAB, W. Messprinzip LV 504. Spannpotentiale ausschöpfen durch eine exakte Längenmessung. *Drahtwelt*. 1994, vol. 3, p. 20-21.

[2] AGAR, W. O. and BLYTHE, I. H. An optical method of measuring transverse surface velocity. *Journal of scientific instruments*. 1968, (I. of physics E), no. 1, p. 25-28.

[3] AIZU, Y. Principles and Development of Spatial Filtering Velocimetry. *Appl. Physics*. 1987, B 43, p.209-224, Springer-Verlag.

[4] ATOR, J.T. Image - velocity sensing with paralell – slit reticles. *Journal of the optical society of America*. 1963, vol. 53 ,p. 1416-1422.

[5] ATOR, J. T. Image velocity sensing by optical correlation. *Applied Optics*. 1966, vol. 5, p. 1325-1331.

[6] BERGELER, S., KRAMBEER, H., MICHEL, K. *Einsatz zweidimensionaler CMOS-Arrays in der Ortsfiltersensorik.* Universität Rostock, Institut für Allgemeine Elektrotechnik.

[7] CORRSYS GmbH. Für schnelle Bandgüter mit neuer gitteroptisch-inteligenter Meß-Sensorik zu neuen Ufern. *Sensor Magazin*.1996, vol. 1, p. 22-23.

[8] COURSEY, M. A Better Roughness Gauge? *Photonics Spectra.* July 2001, p. 125-130.

[9] CZARSKE, J., HOCK, F. Quadrature Demodulation – A new Burstsignal Frequency Estimator. *Laser Anemometry Advances and Applications*. 1993, vol. 2052, pp. 79-86.

[10] ČERMÁK, K., MOHR, F. Adaptive Spatial Filter for Velocity Measurement Devices Based on the Spatial Filter Method. In *Proceeding of ODIMAP IV, 4th Topical Meeting on Optoelectronic Distance/Displacement Measurements and Applications*. University of Oulu, Finland, Kirjapaino OuluPrint OY, 2004, p. 274 - 279, ISBN 951-42-7368-0.

[11] ČERMÁK, K., PROKEŠ, A. Spatial filtering method based velocity measurement – one point surface model. In *Proceedings of the Radioelektronika 2004*. Radioelektronika 2004. Bratislava, Slovak university of Technology in Bratislava, 2004, p. 147 - 150, ISBN 80-227-2017-8.

[12] ČERMÁK, K., MOHR, F. Classification and Optimisation of Velocity Measurement Devices based on Spatial Filtering. In *Proceeding of 8th International Symposium on Measurement and Quality Control in Production*. Düsseldorf, Germany, VDI Verlag GmbH, 2004, p. 669 - 675, ISBN 3-18-091860-8.

[13] ČERMÁK, K., MOHR, F., PROKEŠ, A. Influence of the surface structure properties on the accuracy of the spatial filtering based velocity measurement. In *Proceeding of 14th International Travelling Summer School on Microwaves and Lightwaves ITSS 2004*. Brno, Czech Republic: Dept. of Radio Electronics, FEEC, BUT, 2010, p. 396 – 400.

[14] ČERMÁK, K. Laser Doppler Velocimeter. In *Proceedings of 9th Conference an Competition Student EEICT 2003*. Student EEICT 2003. VUT Brno, 2003, p. 41 - 45, ISBN 80-214-2378-1.

[15] ČERMÁK, K. Laser and Physical Optics Design Software. In *Proceedings of the Radioelektronika 2002*. Radioelektronika 2002. 12th International Czech-Slovak Scientific Conference. Department of Radio and Electronics, FEI SUT Bratislava, 2002, p. 83 - 86, ISBN 80-227-1700-2.

[16] ČERMÁK, K., PROKEŠ, A. Metody pro měření podélné a transverzální rychlosti (Methods for longitudinal and transversal velocity measurement). *Elektrorevue* - Internetový časopis (http://www.elektrorevue.cz). 2003/8, vol. 2, p. 1 – 12, ISSN 1213-1539

[17] ČERMÁK, K. Spatial Filters for Transversal Velocity Measurement. In *Proceedings of the International Conference and Competition Student EEICT 2003*. International Conference and Competition Student EEICT 2003. FEKT, VUT Brno, 2003, p. 46 - 50, ISBN 80-214-2401-X.

[18] ČERMÁK, K., PROKEŠ, A. Velocity measurement method using spatial frequency filtering. In *Proceedings of the Radioelektronika 2003*. 13th International Czech-Slovak Scientific Conference. Radioelektronika 2003. VUT Brno, 2003, p. 471 - 474, ISBN 80-214-2383-8.

[19] ČERMÁK, K. Electro-optical methods of distance and velocity measurement. In *Proceedings of the 8th Conference and Competition Student EEICT 2002*. Student EEICT 2002. VUT Brno, 2002, vol. 3, p. 287 - 291, ISBN 80-214-2116-9.

[20] ČERMÁK, K. Infrared measurement of distance and velocity. In *Proceedings of the 12th International Traveling Summer School on Microwaves and Lightwaves.* 12th International Travelling Summer School on Microwaves and Lightwaves. Institute of Electronics of National Academy of Sciences of Belarus, Institute of Electronics of National Academy of Sciences of Belarus, 2002, p. 234 – 239.

[21] ČERMÁK, K. Ultrazvukový měřič vzdálenosti (Ultrasonic distance finder). In *Proceedings of the 7th conference Student FEI 2001*. vol. 1, Student FEI 2001. FEI VUT Brno, 2001, p. 157 - 159, ISBN 80-214-1859-1.

[22] DELINGATE, E. Berührungslose optische Geschwindigkeits- und Abstandsmessung. *Leitz Mitteilungen für Wissenschaft und Technik*. 1976/4, vol. VI, no. 7.

[23] DOPHEIDE, D., TAUX, G. Geschwindigkeits- und Durchflussmessung mit optoelektronischen Bauelementen. *Technisches Messen*. 6/1985, p. 253-263.

[24] ERNST LEITZ GMBH, *Apparatus for measuring properties of movement*. London Patent Office, 1971, Patent Nr. 1 389 309.

[25] FIEDLER, O., RICHTER, A. Ortsfilter-Geschwindigkeitssensor für industrielle Anwendungen. In *Proceedings of SENSOR 96 congress*. p. 129-134.

[26] FRITSCHE, R. und MESCH, F. Non-contact speed measurement – a comparison of optical systems. *Measurement and Control*. 1973, vol. 6, p. 293-300.

[27] FRITSCHE, R. und MESCH, F. Vergleich von Ortsfrequenzfilterung und Korrelationsverfahren zur berühungslosen Geschwindigkeitsmessung. *Acta IMEKO*. 1973, p. 579-587.

[28] GERALD FITZ, A.S. *Photo Electric System*. 1935, US Patent No.: 2,016,036.

[29] HAIR, T., BLYTHE, J.H. and AGAR, W.O.: An optical method of measuring transverse surface velocity. *Acta IMEKO*, 1967, p. 191-198.

[30] HEITMANN, K., SCHNEIDER, E. *Einrichtung zur berührungslosen Messung*. 1973, Patent Nr. DE 23 30 940.

[31] HEITMANN, K., SCHNEIDER, E., EISENKOPF, H. *Einrichtung zur berühungslosen Messung der relativen Geschwindigkeit, Lage, Entfernung oder Verschiebestrecke von Objekten*. 1974, Patent Nr. CH 548 605.

[32] HENNING, E., MARK, W. *Image Enhancement Using On-Line Spatial Filtering*. 1980, Patent Nr. US 4,238,772.

[33] HOCK, B., HUHNKE, B. Berührungslose Geschwindigkeits- und Längenmessung mit absolutem Meßfehler < 0,1 %. *SENZOR report*. 2/1995, p. 31-32.

[34] HUHNKE, B. Optische Sensorik: Berührungslose Längen- und Geschwindigkeitsmessung mit Richtungserkennung. *Sensor Magazin*. 2/94, p. 13-14.

[35] HUHNKE, B. Kompakter optoelektronischer 2-D Sensor zur Weg-, Geschwindigkeits- und Winkelbestimmung. *Sensor Magazin*. 3/94, p. 12-14.

[36] ITAKURA, Y., SUGIMURA, A. and TSUTSUMI, S. Amplitude-modulated reticle constructed by a liquid crystal cell array. *Applied Optics*. 1981, vol.20, no.16, p. 2819-2826.

[37] KRAMBEER, H., MICHEL, K., CHRISTOFORI, K. *Ortsfilterverfahren zur optischen Messung geringer Geschwindigkeiten von Oberflächen, Partikeln und Strömungen*. Universität Rostock, Institut für Allgemeine Elektrotechnik.

[38] KREUTZER, P. Berührugslose Geschwindigkeitsmessung bei quer zur Meßrichtung verlaufender Bewegung. *Dissertation thesis*. Universität Stuttgart, 1973.

[39] KREUTZER, P. Theoretische Betrachtungen zur berührungslosen Geschwindigkeitsmessung mit optischen Gittern. *Feinwerktechnik und Messtechnik*. 6/1975, p.289-294.

[40] LEITZ, L., KNUT, H., SCHNEIDER, E. *Verfahren und Einrichtungen zur fotoelektrischen Bestimmung der Lage mindestens einer Schärfenebene eines Bildes*. 1973, Patent Nr. DE 21 44 487.

[41] LEITZ, L., KNUT, H., SCHNEIDER, E. *Einrichtung zur berührungslosen Messung*. 1973, Patent Nr. DE 22 09 667.

[42] MESCH, F., DAUCHER and FRITSCHE, R. Geschwindigkeitsmessung mit Korrelationsverfahren. *Meßtechnik*. 1971, vol. 79, p. 152-157 and p. 163-168.

[43] MICHEL, K. C., FIEDLER, O. F., RICHTER, A., CHRISTOFORI, K. and BERGLER, S. A Novel Spatial Filtering Velocimetr Based on Photodetector Array. *IEEE Transactions on Instrumentation and Measurement*. 1998, vol. 47, No. 1.

[44] MICHEL, K. Ein Beitrag zur Signalverarbeitung von Ortsfiltern. *Dissertation thesis*. Universität Rostock, 2000.

[45] MOHR, F. Optical Interferometry – Basics and Technical Applications. In *Proceeding of 14th International Travelling Summer School on Microwaves and Lightwaves ITSS 2004*. Brno, Czech Republic: Dept. of Radio Electronics, FEEC, BUT, 2010, p. 301 – 316.

[46] MOHR, F. Heterodyn-Interferometer zur Vibrationsanalyse. *Technisches Messen.* 1990, vol. 57, p. 335-345.

[47] POKLEKOWSKI, G. und SCHULZ, W. Geschwindigkeitsmessung an Schnelllaufenden Walzstraßen mit Hilfe der Lasertechnik. *Stahl und Eisen*. 1970, vol. 90, no. 17, p. 897-903.

[48] PROKEŠ, A. Correctness of Velocity Evaluation of System Using Spatial Filter. *Radioengineering*, 2002, vol. 11, no. 3, p. 24-26.

[49] PROKEŠ, A., ČERMÁK, K. Využití přímé kmitočtové syntézy v radiotechnice (Direct frequency mixing applications in radiolectronics). *Elektrorevue* - Internetový časopis (http://www.elektrorevue.cz), 2003/48, vol. 12, p. 1 – 10, ISSN 1213-1539.

[50] RUDD, M. J. The laser anemometr – a review. *Optics and Laser Technology*. 1971, p. 200-207.

[51] SCHANZ, M. Eindimensionale CMOS Bildsensorik mit integrierter Signalverarbeitung. *Dissertation thesis*. Gerhard - Mercator - Universität - Gesamthochschule Duisburg, 1998.

[52] SCHRÖDER, C., BERGLER, S., KRAMBEER, H., MICHEL, K. *Erweiterung der Ortsfiltervelocimetrie zur Teilchengrößenmessung*. Universität Rostock, Institut für Allgemeine Elektrotechnik.

[53] SCHULZ, W. Mit Laserlicht gemessen. *Elektrotechnik*. 1975, vol. 57, p. 12-15.

[54] SCHWENZFEIER, W., KAWA, F. Zur Frage der Messgenauigkeit von laseroptischen Geschwindigkeitsmessgeräten im Industrieeinsatz. *Fachberichte Hüttenpraxis Metallverarbeitung*. 1985, vol. 23, no. 11.

[55] SPIES, G., MEYER, H., BOHMANN, J. *A Signal Processor for Non-Contact Speed Measurement of Rail Guided Devices*. Aachen, Technical University (RWTH).

[56] TSUDAGAWA, M., SUGIMOTO, S. and YAMADA, H. An Estimation Method of the Central Frequency for Optical Velocity Sensors. In *Proceedings IEEE Instrumentation and Measurement Technology Conference.* 1989, pp. 450-455.

[57] WEFERS, N. *Verfahren und Vorrichtung zum berührungslosen Bestimmen des Bewegungszustandes eines länglichen Objektes*. 1994, Patent Nr. DE 42 44 521.

[58] WHIPPLE, CH. T. Sensors Keep an Eye on Road Surfaces. *Photonics Spectra*. June 1996.

[59] YASUFUMI AMARI and ISAO MASUDA Velocity Sense Detection Based on the Spatial Filter Method. *IEEE Transactions on Instrumentation and Measurement*. August 1990, vol. 39, no. 4.

[60] ZOMOTER, A. Ein korrelationsoptisches Verfahren zur direkten Messung von instationären Schwimm- und Schräglaufwinkeln an Kraftfahrzeugen. *Automobiltechnische Zeitschrift*. 1975, vol. 77, p. 213-218.

CURRICULUM VITAE

Personal Details

Name:	Ing. Karel Čermák Ph.D.
Address:	Přátelství 2008 Písek 39701 Czech Republic
Email:	cermakk@feec.vutbr.cz
Born:	October 25th 1977 in Písek
Marital Status:	Single

Education

2001/07 – 2005/09	*Doctoral study program* University: Brno University of Technology, Czech Republic Faculty: Electrical Engineering and Communication Study focus: Optical measurement
2002/10 – 2005/03	University: Pforzheim University of Applied Sciences, Germany Faculty: Electronics and Information Science Study focus: Research for the Doctoral thesis.
1996/09 – 2001/06	*Master study program* University: Brno University of Technology, Czech Republic Faculty: Electrotechnics and Computer Sciences Branch of study: Electronics and Communication
2001/02 – 2001/06	*Erasmus study program* University: Wiesbaden University of Applied Sciences, Germany Faculty: Information Technology and Electrical Engineering
1992/09 – 1996/06	*Secondary school* Technical School of Electrical Engineering, Czech Republic

Skills

Languages:	Czech – Mother tongue German – ZMP by Goethe Institute English – Upper-Intermediate Russian – Pre-intermediate
Other:	Contactless measurement methods, sensors, analogue and digital circuit technique, signal processing, optic.

ABSTRACT

In the first part of the dissertation thesis, the reader is familiarized with the state of the art of the optical methods for transversal velocity measurement. The second part of the thesis focuses on the spatial filter design and the analysis of the surface structures with the intention to find an optimum adaptation of the spatial filter to the material surface properties. In this chapter an improved spatial filter is proposed – the dual differential spatial filter. Finally, in the third chapter, the simulated and computed results are verified using a commercial device and an assembled CCD velocity meter, which were both based on the spatial filtering method.

ABSTRAKT

V první části disertační práce je čtenář seznamován se současným stavem optoelektronických metod pro měření transverzální rychlosti, především však s metodou prostorové filtrace. První část druhé kapitoly se zabývá teoretickým popisem a návrhem prostorového filtru. Je prováděna analýza povrchových struktur s následným vyhodnocením. Jsou stanoveny optimalizační kritéria pro potlačení nežádoucích periodických textur povrchu a návrh prostorového filtru. V této kapitole je rovněž navržena a popsána vylepšená verze prostorového filtru - dvojitý diferenciální prostorový filtr. V třetí kapitole jsou prezentovány výsledky měření. Stěžejní výpočty a simulace z druhé kapitoly jsou zde ověřeny na komerčním zařízení a na navrženém měřícím systému využívajícím rychlostní CCD kameru.